

Analysis of the Global Swell Distributions Using ECMWF Re-Analyses Wind Wave Data

ZHANG Jie, WANG Weili, and GUAN Changlong*

Physical Oceanography Laboratory, Ocean University of China, Qingdao 266100, P. R. China

(Received May 6, 2011; revised May 11, 2011; accepted July 1, 2011)

© Ocean University of China, Science Press and Springer-Verlag Berlin Heidelberg 2011

Abstract The existence of three well-defined tongue-shaped zones of swell dominance, termed as ‘swell pools’, in the Pacific, the Atlantic and the Indian Oceans, was reported by Chen *et al.* (2002) using satellite data. In this paper, the ECMWF Re-analyses wind wave data, including wind speed, significant wave height, averaged wave period and direction, are applied to verify the existence of these swell pools. The swell indices calculated from wave height, wave age and correlation coefficient are used to identify swell events. The wave age swell index can be more appropriately related to physical processes compared to the other two swell indices. Based on the ECMWF data the swell pools in the Pacific and the Atlantic Oceans are confirmed, but the expected swell pool in the Indian Ocean is not pronounced. The seasonal variations of global and hemispherical swell indices are investigated, and the argument that swells in the pools seemed to originate mostly from the winter hemisphere is supported by the seasonal variation of the averaged wave direction. The northward bending of the swell pools in the Pacific and the Atlantic Oceans in summer is not revealed by the ECMWF data. The swell pool in the Indian Ocean and the summer northward bending of the swell pools in the Pacific and the Atlantic Oceans need to be further verified by other datasets.

Key words global swell distribution; swell index; wave age; ECMWF Re-analyses data

1 Introduction

The most common ocean waves are the wind-generated surface gravity waves at the air-sea interface. It is believed that the transfer of energy and momentum from wind to current is through waves and is the primary driving forcing for wind-driven ocean circulation (WISE Group, 2007). Wang and Huang (2004) estimated that global wind energy input for the generation of surface gravity waves is 60 TW. Huang and Wang (2006) argued that, even if a small portion of this energy is transported into the sub-surface ocean, it will play a major role in regulating ocean general circulation.

Conventionally, surface gravity waves are classified into two categories, wind waves and swells. The former are formed due to the direct action of local winds and appear more chaotic, while the latter are defined as waves that have traveled out of a storm-generating area. Swells have longer periods and a smoother appearance than wind waves in the storm area. Away from the storm center, long period swells have been observed to propagate over very large distances, up to half-way around the globe (Munk *et al.*, 1963), radiating a large amount of momentum and energy across ocean basins. In the past several

decades, more studies have focused on wind waves than swells. However, swells are gaining increasing concerns because of its potentially destructive consequences on coastal structures and marine activities (Mettlach *et al.*, 1994). Since sea surface roughness is due mainly to surface gravity waves, the presence of swells and wind waves is considered as an important factor in parameterizing the drag coefficient (Donelan *et al.*, 1997; Guan and Xie, 2004).

On the basis of satellite observational data, including wind speed and significant wave height, Chen *et al.* (2002) found that three well-defined tongue-shaped zones of swell dominance, termed ‘swell pools’, were located in the eastern tropical regions of the Pacific, the Atlantic, and the Indian Oceans, respectively. The satellite data they used are distributed unevenly over the world oceans with increasing poleward spatial coverage (see their Fig.2). The criterion used to classify sea states as wind waves or swells is the empirical relation between wind speed and significant wave height adopted in the WAM model for fully developed seas (WAMDI Group, 1988). However, the conventional criterion to classify swells from wind waves is based on wave age in connection with mechanisms for wave generation proposed by Miles (1957). Miles’ (1957) wave generation mechanisms state that the swell component with phase speed faster than wind speed is not able to obtain energy from air flow. Most recently, Collard *et al.* (2009) reported that the swells in the tropi-

* Corresponding author. Tel: 0086-532-66782192
E-mail: clguan@ouc.edu.cn

cal Eastern Pacific Ocean (the swell pool) originated from storms south to New Zealand in the Southern Pacific, using global satellite Synthetic Aperture Radar (SAR) observations. This implies that the formation of the swell pools could be revealed by the global view of wave propagation directions.

In the present paper, the ECMWF Re-analysis wind wave data (hereafter referred to as the ECMWF data) are used to analyze the global distributions of swells based on the following considerations. First, it is necessary to verify whether a swell pool is dependent on datasets used. The ECMWF data are one of the datasets that cover evenly the world oceans. Second, the present ECMWF data include not only wind speed and significant wave height as do the satellite data used by Chen *et al.* (2002), but also averaged wave period and direction. This makes it possible to use the wave age as one of the criteria to classify swells, and the present study can thus verify whether the swell pool pattern is dependent on different criteria. Finally, the formation of the swell pool could be investigated with the wave direction information from the ECMWF data.

2 Data and Methodology

2.1 Data

The ECMWF data provide wind speed at 10-m height, significant wave height, averaged wave period, and direction. The dataset contains model results and satellite data, and is regularly gridded with 1.5° resolution in both longitudinal and latitudinal directions with a 6-hour time interval (Caires *et al.*, 2004). In order to be consistent with Chen *et al.* (2002), only the data generated for the period from January 1997 to December 2001 are used.

2.2 Methodology

Chen *et al.* (2002) used the following empirical relation between wind speed and significant wave height to classify swells from wind waves:

$$H_s = 1.614 \times 10^{-2} U_{10}^2, \quad 0 \leq U_{10} \leq 7.5 \text{ m s}^{-1}, \quad (1a)$$

$$H_s = 10^{-2} U_{10}^2 + 8.134 \times 10^{-4} U_{10}^3, \quad 7.5 \text{ m s}^{-1} < U_{10} \leq 50 \text{ m s}^{-1}, \quad (1b)$$

where U_{10} (in m s^{-1}) is the wind speed at 10-m height above sea surface, and H_s (in m) is the significant wave height. At a given location with concurrent measurements of wind speed and significant wave height, Chen *et al.* (2002) defined the sea state as the swells if the significant wave height is greater than that predicted by Eq. (1), while the sea state is considered as a growing sea in case the significant wave height is less than that predicted by Eq. (1). As pointed out by Chen *et al.* (2002), this inference is not supposed to be valid in an absolute sense due to the complexity of the wind wave-swell coupling. But it is expected to give a meaningful classification of the two regimes from a statistical point of view. In order to quan-

tify frequencies of swell and wind wave occurrences, two probability indices are introduced by Chen *et al.* (2002):

$$P_s = N_s / N, \quad (2a)$$

$$P_w = N_w / N, \quad (2b)$$

where N_s and N_w are the numbers of swell and wind wave events, respectively, at a given location during a certain time period. Note that the total number $N = N_s + N_w$, thus $P_s + P_w = 1$. Obviously, the values of P_s and P_w vary spatially and temporally.

Besides Eq. (1), the wave age is an alternative parameter to classify swells from wind waves, and can be defined as

$$\beta = \frac{C}{U} = \frac{gT}{2\pi U}, \quad (3)$$

where C and T are the phase velocity and the period of any kinds of waves, respectively, U the wind speed at a height above sea surface, and g the gravitational acceleration. Note that the dispersion relation for deep water waves is used in Eq. (3). In the ECMWF data, the averaged period is defined as

$$T = T_{-1,0} = 2\pi \frac{m_{-1}}{m_0}, \quad (4)$$

where m_r (r is an integer) is the r -th order moment of wave spectrum, defined as

$$m_r = \int_0^{\infty} \omega^r S(\omega) d\omega, \quad (5)$$

and ω is the angular frequency and $S(\omega)$ the wave frequency spectrum.

Using the averaged period calculated by Eq. (4), the wave age could be obtained from the P-M spectrum (Pierson and Moskowitz, 1964) as follows:

$$\beta_{PM} = 0.9773, \quad (6)$$

which defines a critical value for classifying swells and wind waves. At a given geographical location, the sea state is considered as the swell if the wave age by Eq. (3) is greater than β_{PM} , while the sea state is the growing wind wave if it is less than β_{PM} . Similarly, the probability indices for the wave age criterion could be calculated by Eq. (2). Because the 19.5 m level wind is used in the P-M spectrum, the ECMWF wind data are converted to the 19.5-m level to compute the probability indices of swells and wind waves. In the course of wind speed conversion, Wu's (1980) formula is used, namely,

$$C_d = (0.8 + 0.065U_{10}) \times 10^{-3}, \quad (7)$$

where C_d is the drag coefficient and U_{10} is the 10-m level wind speed (m s^{-1}).

A fetch law for the wind wave state (Guan and Sun, 2004) indicates that significant wave height is highly

correlated with wind speed, therefore the correlation coefficient between significant wave height and wind speed is a statistical measure of the sea state. A large correlation value is mostly corresponding to growing waves, while a small value to the swell-dominated state.

Three swell indices will be calculated to verify the swell pool pattern in this study. Two swell probability indices are based respectively on the relationship between wind speed and wave height, and on the wave age, and the third one is based on the correlation coefficient between wind speed and wave height, which is also referred to as the correlation coefficient index.

3 Results

3.1 Swell Climate and Swell Pools

Following the methodology described in Section 2, the annual variation of global swell distribution is examined by calculating the two swell probability indices and the correlation coefficient index. Comparisons are made between the three indices, and the seasonal variation of global swell distribution is studied using one of the three indices. For simplicity and clarity, the swell probability index from the wind speed and wave height relation is referred as the swell index of wave height, and the swell probability index from the wave age is referred as the swell index of wave age. The calculated results of global swell indices are shown in Fig.1 and the climatologies of wind speed and significant wave height are shown in

Fig.2.

Qualitatively, the index distribution patterns in Figs.1a, 1b, and 1c are similar, with two well-defined swell pools located in the tropical and subtropical areas near the eastern Pacific and Atlantic Oceans. However, the swell pool in the Indian Ocean, mentioned in Chen *et al.*'s study (2002), is not pronounced. Because the same swell probability index is used as that in Chen *et al.* (2002), this study shows that the two swell pools in the Pacific and the Atlantic Oceans are more robust than that in the Indian Ocean by comparing the three similar swell pools identified by Chen *et al.* (2002). The existence of the swell pool in the Indian Ocean is somewhat data-dependent. As pointed out by Chen *et al.* (2002), the index patterns in Figs.1a–c show little similarity to that of the wind speed or wave height climatology. In fact, there is little similarity between the spatial patterns of wind speed and wave height climatologies in low and mid-latitudes either (Figs.2a and 2b), which implies that the formation of swell pools is likely due to the swell propagation from high latitudes (Kinsman, 1965; Collard *et al.*, 2009).

Surprisingly to some extent, the range of values of swell index of wave age is much wider than that of swell index of wave height. So the former swell index is more convenient than the latter to depict the swell distribution numerically. In addition, considering the physical process in wind wave generation, the swell index of wave age will be employed in the next subsection to investigate the seasonal variation of global swell distribution.

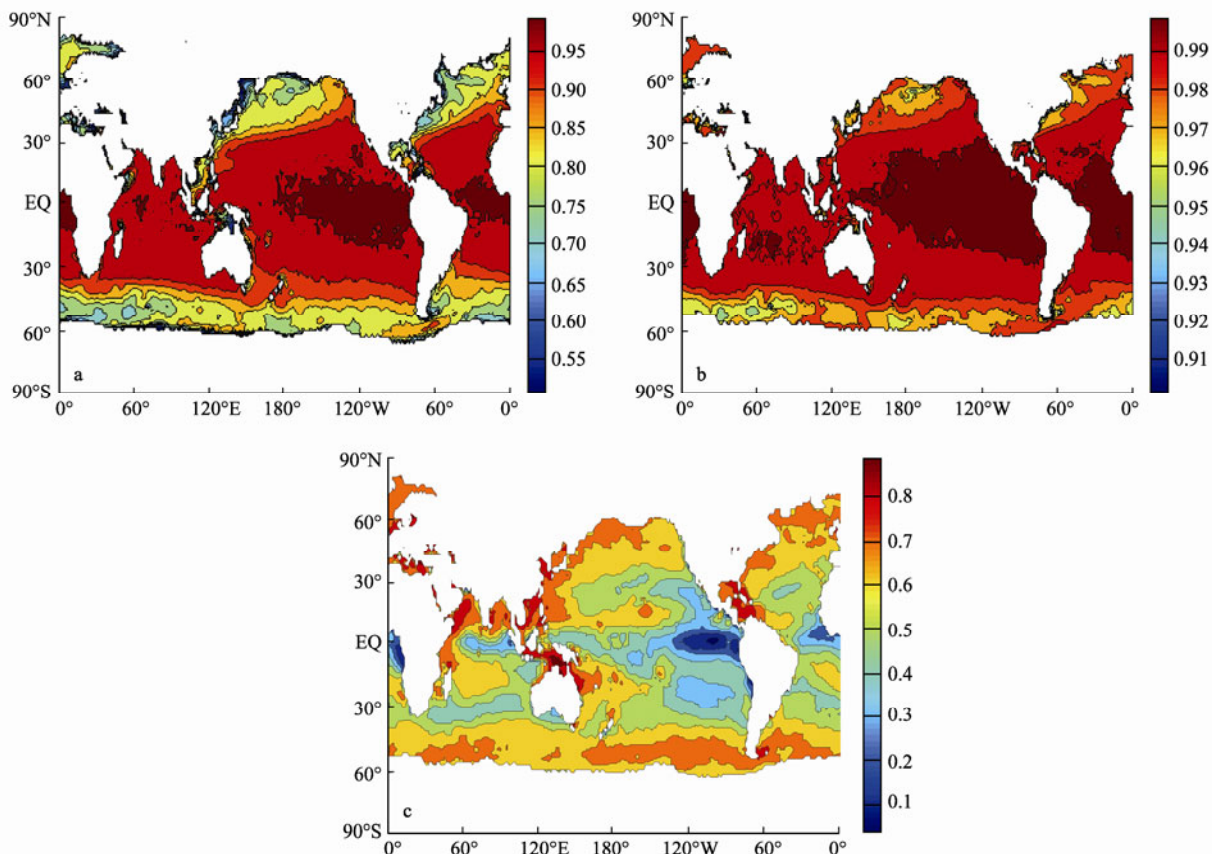


Fig.1 Global distributions of swell indices calculated from (a) wave age, (b) wave height, and (c) correlation coefficient.

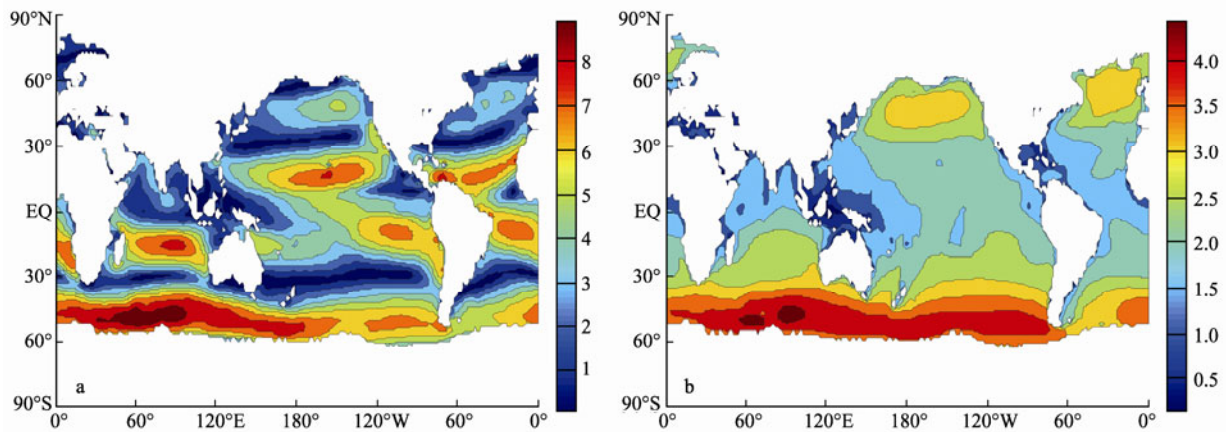


Fig.2 Global distributions of (a) wind speed and (b) significant wave height.

3.2 Seasonal Variation

The seasonal variations of global and hemispherical swell indices are shown in Table 1 (seasons refer to the Northern Hemisphere unless otherwise specified). As is similar to what Chen *et al.* (2002) reported, the swell occurrence undergoes an opposite annual cycle for the Northern and the Southern Hemispheres. In the Northern Hemi-

sphere the swell index reaches the maximum value in summer and the minimum in winter. The winter maximum and the summer minimum are observed for the Southern Hemisphere.

Chen *et al.* (2002) indicated that swell pools seem to get their swells mostly from the winter hemisphere. As shown by the seasonal variation of the global distribution of the averaged wave direction in Fig.3, the prevailing

Table 1 Seasonal variations of global and hemispherical swell indices calculated from the wave age

Season (Months)	Spring (MAM)	Summer (JJA)	Autumn (SON)	Winter (DJF)	Total
Northern Hemisphere	0.88324	0.9232	0.90087	0.86151	0.8922
Southern Hemisphere	0.92525	0.89746	0.9005	0.93005	0.9133
Global	0.9042	0.9103	0.9007	0.8958	0.9027

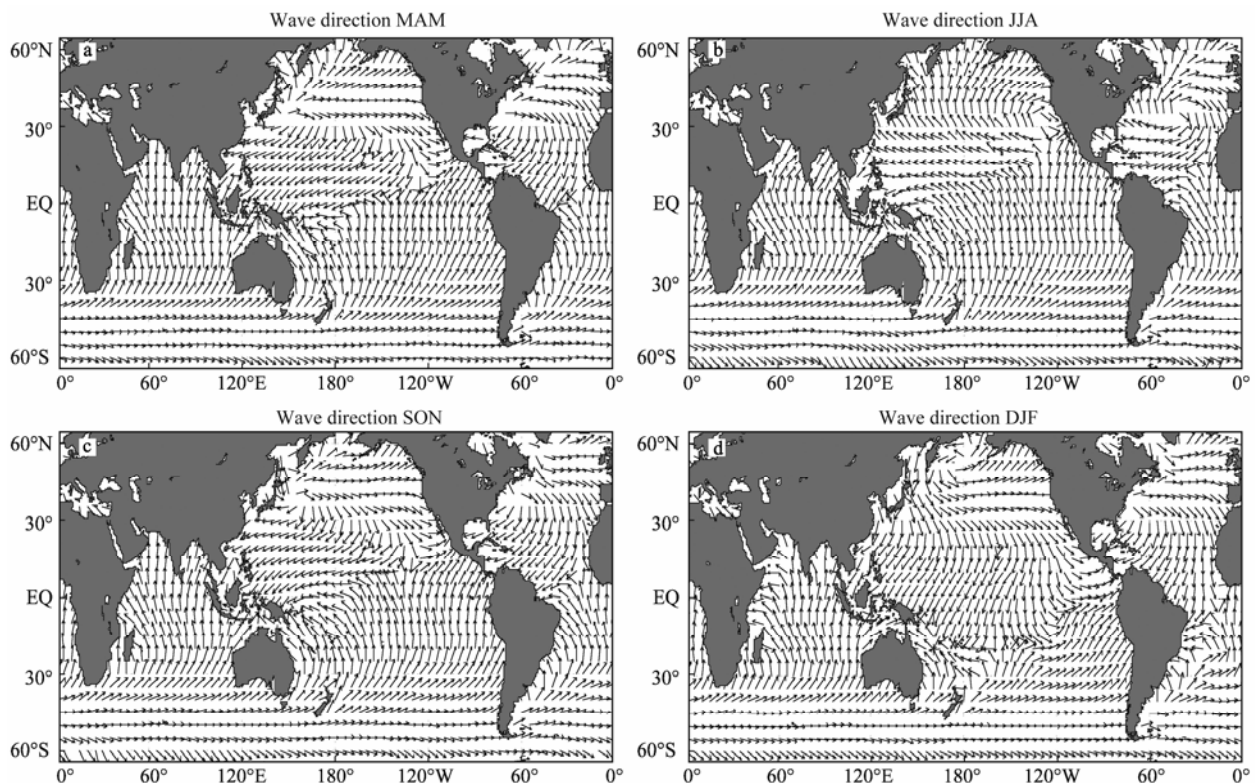


Fig.3 Global distributions of the averaged wave direction for (a) spring (MAM), (b) summer (JJA), (c) autumn (SON), and (d) winter (DJF).

wave directions in the Pacific and the Atlantic Oceans are from the Northern Hemisphere (winter hemisphere) in winter, while waves propagate from the Southern Hemisphere (winter hemisphere) in summer. The prevailing wave directions are northward in the India Ocean in all seasons, which provides a plausible explanation for the absence of the swell pool in the Indian Ocean.

Fig.4 shows the global swell index distribution for each season. It is obvious that the swell pools are well-defined in the Pacific and the Atlantic Oceans, while the swell

pool is not pronounced in the Indian Ocean for all four seasons. In addition, the northward bending of the swell pools in the Pacific and the Atlantic Oceans during summer, which is reported by Chen *et al.* (2002) as the most striking seasonal feature of the swell pools, cannot be observed using the present datasets. This northward bending phenomenon as well as the existence and variation of the swell pool in the Indian Ocean still needs to be verified with other datasets, for instance, the ECMWF ERA-40 Re-analyses wind wave data.

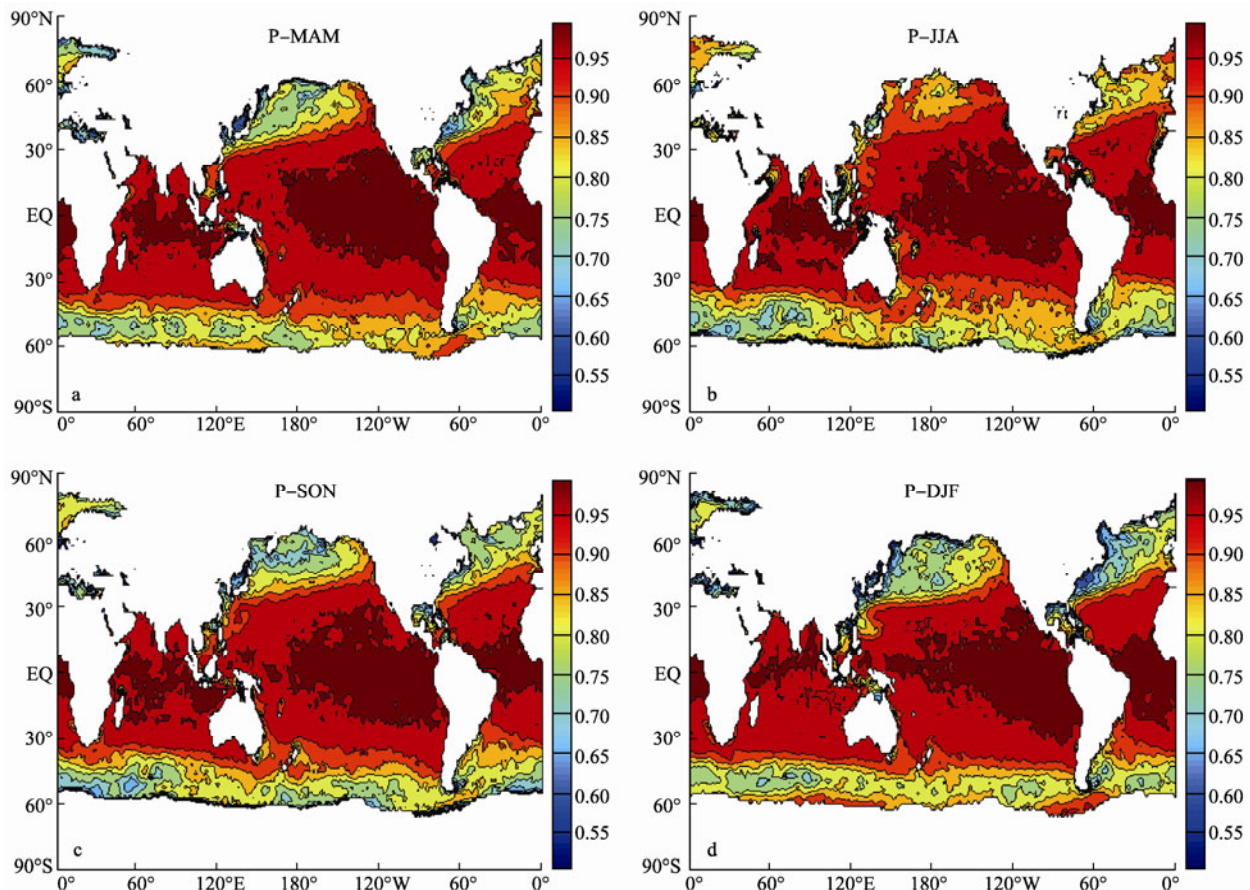


Fig.4 Global distributions of the swell index calculated from wave age for (a) spring (MAM), (b) summer (JJA), (c) autumn (SON), and (d) winter (DJF).

4 Summary

In this paper, the ECMWF Re-analyses wind wave data are applied to investigate the global swell index distribution. Three different criteria for classifying the swells from wind waves are analyzed to examine the three swell pools in the world oceans. It is indicated that the swell index of wave age is more applicable and of physical significance. The ECMWF data verify the existence of the swell pools in the Pacific and the Atlantic Oceans and do not show any swell pool in the Indian Ocean. The seasonal variations of global and hemispherical swell indices are confirmed, and the argument that swell pools seem to obtain the swells mostly from the winter hemisphere is supported by the seasonal variation of the averaged wave direction. However, the swell pool in the Indian Ocean and the northward bending of the swell pools in the Pa-

cific and the Atlantic Oceans in summer need further verification with different datasets.

Acknowledgements

The authors appreciate the support from the National Natural Science Foundation of China (Nos. 40830959 and 40921004) and from the Ministry of Science and Technology of China (No. 2011BAC03B01).

References

- Caires, S., Sterl, A., Bidlot, J.-R., Graham, N., and Swail, V., 2004. Intercomparison of different wind wave reanalyses. *Journal of Climate*, **17**: 1893-1913.
- Chen, G., Chapron, B., Ezraty, R., and Vandemark, D., 2002. A global view of swell and wind sea climate in the ocean by

- satellite altimeter and scatterometer. *Journal of Atmospheric and Oceanic Technology*, **19**: 1849-1859.
- Collard, F., Ardhuin, F., and Chapron, B., 2009. Monitoring and analysis of ocean swell fields from space: New methods for routine observations. *Journal of Geophysical Research*, **114**, C07023, Doi: 10.1029/2008JC005215.
- Donelan, M. A., Drennan, W. M., and Katsaros, K. B., 1997. The air-sea momentum flux in conditions of wind sea and swell. *Journal of Physical Oceanography*, **27**: 2087-2099.
- Guan, C., and Sun, J., 2004. Similarities of some wind input and dissipation source terms. *China Ocean Engineering*, **18** (4): 629-642.
- Guan, C., and Xie, L., 2004. On the linear parameterization of drag coefficient over sea surface. *Journal of Physical Oceanography*, **34**: 2847-2851.
- Huang, R. X., and Wang, W., 2006. Decadal variability of wind-energy input to the world ocean. *Deep-Sea Research II*, **53**: 31-41.
- Kinsman, B., 1965. *Wind Waves*. Printice-Hall, 676pp.
- Mettlach, T., Wang, D., and Wittmann, P., 1994. Analysis and prediction of ocean swell using instrumented buoys. *Journal of Atmospheric and Oceanic Technology*, **11**: 506-524.
- Miles, J. W., 1957. On the generation of surface wave by shear flow. *Journal of Fluid Mechanics.*, **3** (2): 185-204.
- Munk, W. H., Miller, G. R., Snodgrass, F. E., and Barber, N. F., 1963. Directional recording of swell from distant storm. *Philosophical Transactions of the Royal Society of London*, **A255**: 505-584.
- Pierson, W. J., Jr., and Moskowitz, L., 1964. A proposed spectral form for fully developed wind seas based on the similarity theory of S. A. Kitaigorodskii. *Journal of Geophysical Research*, **69** (24): 5181-5203.
- WAMDI Group, 1988. The WAM model – a third generation ocean wave prediction model. *Journal of Physical Oceanography*, **18**: 1775-1809.
- Wang, W., and Huang, R. X., 2004. Wind energy input to the surface waves. *Journal of Physical Oceanography*, **34**: 1276-1280.
- WISE Group, 2007. Wave modelling – The state of the art. *Progress in Oceanography*, **75**: 603-674, Doi: 10.1016/j.pocean.2007.05.005.
- Wu, J., 1980. Wind-stress coefficients over sea surface near neutral conditions – A revisit. *Journal of Physical Oceanography*, **10**: 727-740.

(Edited by Xie Jun)